Am J Cancer Res 2026;16(6):2389-2406
www.ajcr.us /ISSN:2156-6976/ajcr0172936

Original Article

Kang Ru Plus reverses osimertinib resistance in lung adenocarcinoma via suppression of EGFR/PI3K/AKT signaling

Thomas G Mhone[1,13], Wei-Wen Kuo[2,3], Chih-Ying Chi[1], Chia-Hua Kuo[4,5,6], Tsung-Jung Ho[7,8], Yu-Ling Wu[1], Yueh-Min Lin[9,10], Ming-Cheng Chen[11,12], Chih-Yang Huang[1,13,14,15,16,17*], Shinn-Zong Lin[18,19*]

[1]Cardiovascular and Mitochondrial Related Disease Research Center, Hualien Tzu Chi Hospital, Buddhist Tzu Chi Medical Foundation, Hualien, Taiwan; [2]Department of Biological Science and Technology, College of Life Sciences, China Medical University, Taichung, Taiwan; [3]School of Pharmacy, China Medical University, Taichung, Taiwan; [4]Laboratory of Exercise Biochemistry, The Education University of Hong Kong, New Territories, Hong Kong; [5]Soochow University, School of Physical Education and Sports Science, Suzhou, Jiangsu, China; [6]Department of Movement Sciences and Sports Training, School of Sport Sciences, University of Jordan, Jordan; [7]Integration Center of Traditional Chinese and Modern Medicine, Hualien Tzu Chi Hospital, Buddhist Tzu Chi Medical Foundation, Hualien, Taiwan; [8]Department of Chinese Medicine, Hualien Tzu Chi Hospital, Buddhist Tzu Chi Medical Foundation, Hualien, Taiwan; [9]School of Medicine, Chung Shan Medical University, Taichung 402, Taiwan; [10]Department of Pathology, Changhua Christian Hospital, Changhua, Taiwan; [11]Division of Colorectal Surgery, Department of Surgery, Taichung Veterans General Hospital, Taichung 40705, Taiwan; [12]College of Medicine, National Yang Ming Chiao Tung University, Taiwan; [13]Center for Molecular Medicine in Traditional Chinese Medicine, E-Da Hospital, E-Da Healthcare Group, Kaohsiung, Taiwan; [14]School of Chinese Medicine for Post Baccalaureate, I-Shou University, Kaohsiung, Taiwan; [15]Graduate Institute of Biomedical Sciences, China Medical University, Taichung 404, Taiwan; [16]Department of Medical Research, China Medical University Hospital, China Medical University, Taichung 404, Taiwan; [17]Department of Biotechnology, Asia University, Taichung 413, Taiwan; [18]Buddhist Compassion Relief Tzu Chi Foundation, Hualien 970, Taiwan; [19]Department of Neurosurgery, Hualien Tzu Chi Hospital, Hualien, Taiwan. [*]Equal contributors.

Received March 28, 2026; Accepted May 10, 2026; Epub June 15, 2026; Published June 30, 2026

Abstract: Background: Acquired resistance to epidermal growth factor receptor (EGFR) tyrosine kinase inhibitors such as osimertinib remains a major challenge in the treatment of EGFR-mutant non-small cell lung cancer (NSCLC). Multi-component natural product therapies may provide complementary strategies capable of modulating multiple signaling pathways involved in therapeutic resistance. This study investigated the pharmacological activity of Kang Ru Plus (KR-Plus), a multi-herb formulation, and evaluated its ability to enhance sensitivity to osimertinib in resistant lung adenocarcinoma models. Methods: The anti-proliferative and chemosensitizing effects of KR-Plus were assessed in EGFR-mutant lung adenocarcinoma cells and osimertinib-resistant derivatives using MTT assays, flow cytometry, immunofluorescence, and Western blot. Phytochemical composition was characterized by UHPLC-QTOF-MS-based metabolite profiling. Network pharmacology and molecular docking analyses were performed to predict potential targets and pathways. In vivo efficacy was evaluated in H1975-OSR xenograft mouse models. Results: KR-Plus inhibited cell proliferation across multiple cancer cell lines and significantly enhanced the cytotoxic effects of osimertinib in resistant lung adenocarcinoma cells. Mechanistically, KR-Plus reduced EGFR phosphorylation and suppressed downstream PI3K/AKT, ERK, and mTOR signaling, resulting in cell-cycle arrest and apoptosis. Metabolite profiling identified several flavonoids and phenolic compounds with predicted interactions within EGFR-associated signaling networks. In xenograft models, combined treatment with KR-Plus and osimertinib markedly suppressed tumor growth and improved survival without evident systemic toxicity. Conclusion: KR-Plus exerts multi-target effects that disrupt EGFR-driven survival signaling and enhance responsiveness to osimertinib in resistant lung adenocarcinoma models. These findings support the potential of polyherbal formulations as complementary strategies to overcome resistance to targeted therapies.

Keywords: Kang Ru Plus, lung adenocarcinoma, osimertinib resistance, EGFR signaling, apoptosis, phytochemical profiling, network pharmacology

https://doi.org/10.62347/CURF9339

Introduction

Lung cancer remains the leading cause of cancer-related mortality worldwide, with non-small cell lung cancer (NSCLC) accounting for approximately 85% of cases [1]. Aberrant activation of epidermal growth factor receptor (EGFR) signaling is a key oncogenic driver in a substantial proportion of NSCLC patients, and EGFR-targeted therapies have markedly improved clinical outcomes. Third-generation EGFR tyrosine kinase inhibitors, such as osimertinib, have shown significant efficacy in EGFR-mutant disease; however, the development of acquired resistance continues to limit long-term therapeutic benefit [2, 3]. This resistance arises through multiple mechanisms, including activation of compensatory pathways such as PI3K/AKT, MAPK/ERK, and mTOR, along with reduced apoptotic responsiveness and enhanced pro-survival signaling [4-10]. The complexity of these networks underscores the need for therapeutic strategies that can simultaneously target multiple molecular pathways.

Natural products and medicinal plant-derived compounds have long been a rich source of bioactive molecules in cancer therapy. Accumulating evidence shows that phytochemicals can modulate key oncogenic signaling pathways, including EGFR-associated networks that regulate tumor growth, survival, and drug resistance. In particular, flavonoids, phenolic compounds, and related metabolites have been reported to inhibit PI3K/AKT and MAPK signaling, promote apoptosis, and enhance the efficacy of anticancer agents [8, 10]. Against this background, multi-component herbal formulations may offer a pharmacological advantage by concurrently targeting multiple pathways implicated in therapeutic resistance.

Traditional herbal medicine systems have long used polyherbal formulations to manage chronic pulmonary disorders associated with persistent inflammation and impaired respiratory function. Several medicinal plants commonly employed in East Asian medicine for lung-related conditions have demonstrated anti-inflammatory, antioxidant, and anti-proliferative activities in modern pharmacological studies. For example, *Houttuynia cordata* Thunb. exhibits anti-inflammatory and anticancer effects, including modulation of PI3K/AKT signaling. *Artemisia argyi* H.Lév. & Vaniot has shown anti-inflammatory and cytoprotective properties, while *Phyllanthus urinaria* L. displays antitumor and antioxidant activities in experimental models. Additional species, including *Anisomeles indica* (L.) Kuntze and *Lycium barbarum* L., are rich in bioactive phytochemicals with reported anti-inflammatory, immunomodulatory, and anti-proliferative effects [11-16]. Collectively, these plants contain diverse classes of secondary metabolites - such as flavonoids, phenolic acids, terpenoids, and polysaccharides - many of which are known to modulate signaling pathways relevant to tumor growth and survival.

Polyherbal formulations, composed of multiple medicinal plants, may exert synergistic effects through coordinated modulation of cellular signaling networks. Accordingly, growing attention has focused on their potential as complementary strategies in cancer therapy, particularly for overcoming drug resistance. Recent studies show that multi-component herbal preparations can simultaneously regulate key oncogenic pathways, including EGFR, STAT3, PI3K/AKT, and MAPK signaling cascades [17-22]. This multi-target activity may offer advantages over single-compound approaches when addressing the complexity of resistance mechanisms. However, despite increasing interest in plant-derived modulators of EGFR signaling, the potential of polyherbal formulations to overcome resistance to third-generation EGFR inhibitors remains largely underexplored.

Kang Ru Plus (KR-Plus) is a five-herb formulation comprising *Houttuynia cordata*, *Anisomeles indica*, *Phyllanthus urinaria*, *Artemisia argyi*, and *Lycium barbarum*, all of which have been traditionally used to manage pulmonary disorders. These plants are supported by pharmacological evidence demonstrating anti-inflammatory, antioxidant, and antitumor activities. While the bioactive properties of individual components have been investigated, the collective pharmacological effects of this multi-component formulation - particularly in the context of resistance to EGFR-targeted therapies - remain poorly defined.

Accordingly, this study investigated the anti-proliferative and chemosensitizing effects of Kang Ru Plus (KR-Plus) in EGFR-mutant lung adenocarcinoma models with acquired resistance to osimertinib. An integrated approach

was employed, combining in vitro drug-resistant cell models, in vivo xenograft studies, and UHPLC-QTOF-MS-based metabolite profiling with network pharmacology analysis to elucidate the underlying molecular mechanisms. These findings provide insight into the potential of multi-target natural product strategies to overcome therapeutic resistance in EGFR-driven lung cancer.

Materials and methods

Preparation of Kang Ru Plus extract

The five medicinal plants used in Kang Ru Plus (KR-Plus) were selected based on their traditional indications for pulmonary disorders. The formulation comprised the aerial parts of *Anisomeles indica* (L.) Kuntze (Lamiaceae), aerial parts of *Houttuynia cordata* Thunb. (Saururaceae), whole plant of *Phyllanthus urinaria* L. (Phyllanthaceae), leaves of *Artemisia argyi* H.Lév. & Vaniot (Asteraceae), and fruits of *Lycium barbarum* L. (Solanaceae). All crude botanical materials were obtained from the Department of Traditional Chinese Medicine, Hualien Tzu Chi Hospital (Hualien, Taiwan), and authenticated according to pharmacopeial standards used in clinical herbal practice.

The combined herbs were subjected to aqueous reflux extraction at a solvent-to-material ratio of 1:10 (w/v) at 100°C for 2 h, consistent with conventional decoction methods in traditional Chinese medicine. The extract was filtered through Whatman No. 1 filter paper, concentrated under reduced pressure, and lyophilized. The resulting freeze-dried extract was stored at -80°C until use.

For in vitro experiments, the lyophilized powder was reconstituted in sterile distilled water or dimethyl sulfoxide (DMSO) to prepare stock solutions. Working concentrations (250-1000 μg/mL) were freshly prepared for each experiment. This concentration range was selected based on preliminary cytotoxicity screening and to approximate pharmacologically relevant exposure relative to crude herb intake after normalization to extract yield. The final DMSO concentration did not exceed 0.1% (v/v) in cell-based assays. Voucher specimens of all plant materials were deposited in the herbarium of the Department of Traditional Chinese Medicine, Hualien Tzu Chi Hospital, Taiwan.

Cell culture, drug treatments and generation of resistance

A549, H1975, U-118 MG, MCF7, and MDA-MB-231 cell lines were obtained from the American Type Culture Collection (ATCC, Manassas, VA, USA). LoVo, HA22T/VGH, and U-87 MG cells were purchased from the Bioresource Collection and Research Center (BCRC, Hsinchu, Taiwan). A549, A549-OSR, MCF7, and MDA-MB-231 cells were cultured in high-glucose Dulbecco's Modified Eagle Medium (DMEM), while H1975 and H1975-OSR cells were maintained in RPMI-1640. U-118 MG, LoVo, HA22T/VGH, and U-87 MG cells were cultured in DMEM/F-12 medium. All media were supplemented with 10% fetal bovine serum (FBS) and 1% penicillin-streptomycin. Cells were maintained at 80-90% confluence prior to passaging or experimental seeding.

Cells were treated with KR-Plus (250-1000 μg/mL), osimertinib (1-20 μM), or their combination. These models were used to evaluate the cytoregulatory effects of KR-Plus, including its potential to enhance sensitivity to targeted therapy in drug-resistant contexts.

Osimertinib-resistant derivatives were generated by long-term, stepwise exposure of parental A549 and H1975 cells to increasing concentrations of osimertinib. Cells were initially treated with 2.5 μM osimertinib, and the concentration was gradually escalated over approximately 11 months as cells adapted and regained stable proliferation. Dose increments were introduced only after recovery of normal growth kinetics at each step. Resistance was defined as a ≥3-fold increase in IC_{50} relative to the corresponding parental cell line, as determined by MTT assays. Resistant populations were subsequently isolated by single-cell cloning and expanded for further study. The resulting cell lines, designated A549-OSR and H1975-OSR, were maintained in medium containing low-dose osimertinib and cultured without drug for at least two passages prior to experimentation as previously demonstrated [23].

Cell viability

Cell viability was assessed using the MTT assay. Briefly, cancer cells were seeded in 96-well plates and treated with increasing concentrations of KR-Plus or osimertinib (OS) for 24 or 48

h. Following treatment, MTT solution (0.5 mg/mL) was added to each well, and the plates were incubated at 37°C for 2 h. The resulting formazan crystals were dissolved in dimethyl sulfoxide (DMSO), and absorbance was measured at 595 nm using a microplate reader (SpectraMax® ABS Plus, Molecular Devices, USA).

IC_{50} values were determined by fitting the dose-response data using nonlinear regression (log[inhibitor] vs. normalized response, variable slope model) in GraphPad Prism. This approach generates a sigmoidal dose-response curve and allows accurate estimation of IC_{50} values along with 95% confidence intervals.

For combination studies, cells were pretreated with osimertinib for 24 h, followed by co-treatment with KR-Plus for an additional 48 h. Drug interactions were evaluated by calculating combination indices (CI) using CompuSyn software. CI values were interpreted as follows: CI < 1, synergism; CI = 1, additive effect; and CI > 1, antagonism [24, 25].

Whole cell lysate protein extraction and protein quantification

Total cellular proteins were extracted using radioimmunoprecipitation assay (RIPA) lysis buffer supplemented with protease and phosphatase inhibitors, following standard protocols [25]. Cell lysates were collected and stored at -80°C until further analysis.

Protein concentration was determined using the Bradford assay. Briefly, 20 µL of each protein sample or serially diluted bovine serum albumin (BSA) standards (1 mg/mL) were mixed with Coomassie Brilliant Blue reagent and incubated according to the manufacturer's instructions. Absorbance was measured at 595 nm using a microplate reader. Protein concentrations were calculated from a standard curve generated using BSA standards [24].

Western blot analysis

Equal amounts of protein (30-50 µg), quantified as described above, were denatured in 5× sample buffer at 95°C for 5-10 min. Samples were separated by 7-15% SDS-polyacrylamide gel electrophoresis (SDS-PAGE) and transferred onto polyvinylidene fluoride (PVDF) membranes. Membranes were blocked with 5% non-fat milk and incubated overnight at 4°C with primary antibodies against EGFR, phospho-EGFR (p-EGFR), PI3K, AKT, ERK, mTOR, BAX, Bcl-2, caspase-3, PARP, p53, p21, p16, and PCNA. After washing, membranes were incubated with appropriate secondary antibodies for 1 h at room temperature. Protein bands were detected using the Fuji LAS-3000 imaging system.

Apoptosis assays

Apoptosis was quantified using an Annexin V-FITC/propidium iodide (PI) double-staining assay (BD Biosciences) according to the manufacturer's instructions. Briefly, H1975-OSR cells (1×10^6 cells per dish) were seeded in 10 cm dishes and subjected to the indicated treatments. Cells were then harvested by trypsinization, collected by centrifugation, and resuspended in binding buffer containing Annexin V-FITC and PI. Stained cells were analyzed by flow cytometry using a BD FACSCanto II system.

Apoptotic cell populations were quantified as the percentage of early and late apoptotic cells relative to the total cell population.

Cell cycle distribution analysis

Cell cycle distribution was assessed by propidium iodide (PI) staining followed by flow cytometry. Briefly, treated and control cells were harvested by trypsinization, washed with phosphate-buffered saline (PBS), and fixed in cold 70% ethanol at -20°C for at least 30 min or overnight. Following fixation, cells were washed to remove residual ethanol and incubated with staining solution containing PI (50 µg/mL) and RNase A (100 µg/mL) in PBS.

DNA content was analyzed using a BD FACSCanto II flow cytometer, and cell cycle distribution (G0/G1, S, and G2/M phases) was determined from DNA content histograms, as previously described [24].

Immunofluorescence staining

Immunofluorescence staining for proliferating cell nuclear antigen (PCNA) and phosphorylated EGFR (p-EGFR) were performed following standard protocols. Cells were fixed in 4% formaldehyde, permeabilized with 0.2% Triton X-100, and blocked with 10% goat serum for 1 h

at room temperature. Cells were then incubated overnight at 4°C with primary antibodies diluted 1:500 in 1% goat serum.

After washing, cells were incubated with Alexa Fluor 488-conjugated goat anti-rabbit secondary antibody (1:500 in 1% goat serum) for 1 h at room temperature. Nuclei were counterstained and mounted using Fluoroshield mounting medium containing DAPI. Fluorescence images were acquired using a fluorescence microscope.

In vivo xenograft model

Male NU/NU nude mice (6 weeks old) were obtained from BioLASCO Taiwan Co., Ltd. (Taipei, Taiwan) and housed under standard conditions at the Laboratory Animal Service Center (LASC), China Medical University (CMU), in accordance with institutional guidelines and the principles of the 3Rs (Replacement, Reduction, and Refinement) for the humane care and use of laboratory animals [24]. All procedures were approved by the Institutional Animal Care and Use Committee (IACUC) of CMU (approval no. CMUIACUC-2024-200).

For tumor establishment, mice were subcutaneously injected with 5×10^6 H1975-OSR cells suspended in Matrigel and serum-free medium (BD Biosciences). When tumors reached approximately 500 mm^3, mice were randomly assigned to four groups (n = 4 per group): vehicle control, KR-Plus (500 mg/kg/day, oral gavage), osimertinib (25 mg/kg/day, oral gavage), or combination treatment. Tumor growth was monitored every 3 days using caliper measurements, and tumor volume was calculated using the standard formula [24, 25].

Animals were closely monitored throughout the study for general health and signs of distress, including changes in body weight, posture, grooming behavior, mobility, water intake, and overall physical condition. Humane endpoints were predefined based on tumor burden and animal welfare criteria. Mice were euthanized when tumor volume reached 1500 mm^3 or earlier if signs of distress, impaired mobility, or deterioration in general condition were observed.

After 4 weeks of treatment, mice were euthanized, and tumors were excised for histological and biochemical analyses. Serum levels of toxicity markers, including blood urea nitrogen (BUN), glutamate oxaloacetate transaminase (GOT), glutamate pyruvate transaminase (GPT), and total bilirubin (T-Bil), were measured using an automated biochemical analyzer.

LC-MS metabolite profiling

KR-Plus extract was analyzed using ultra-high-performance liquid chromatography coupled with quadrupole time-of-flight mass spectrometry (UHPLC-QTOF-MS; Agilent 1290 Infinity II LC system coupled to a 6545 QTOF mass spectrometer). Chromatographic separation was performed on a C18 column using a gradient elution of water (0.1% formic acid) and acetonitrile.

Mass spectrometry data were acquired in positive ionization mode. Metabolites were annotated based on accurate mass matching against public databases, including the Human Metabolome Database (HMDB), METLIN, and MassBank. Identified compounds were subsequently evaluated for their reported anticancer activities and potential relevance to EGFR-associated signaling pathways [26].

Target prediction and pathway analysis

Identified metabolites were subjected to target prediction using SwissTargetPrediction (https://www.swisstargetprediction.ch/). Molecular docking analyses were subsequently performed using the Attracting Cavities (Attracting Cavities) algorithm to evaluate potential ligand-protein interactions [27]. Pathway enrichment analysis was conducted based on the KEGG 2021 Human database, while protein-protein interaction (PPI) networks were constructed using the STRING database and visualized with Enrichr [28]. Three-dimensional structures of EGFR and related signaling proteins, including PI3K, AKT, and mTOR, were obtained from the Protein Data Bank (PDB; https://www.rcsb.org/) and used to validate docking interactions and assess binding site occupancy.

Statistical analysis

Statistical analyses were performed using one-way or two-way analysis of variance (ANOVA), as appropriate, followed by relevant post hoc tests. Differences were considered statistically significant at $P < 0.05$. All experiments were conducted in triplicate, and data are presented as mean ± standard deviation (SD).

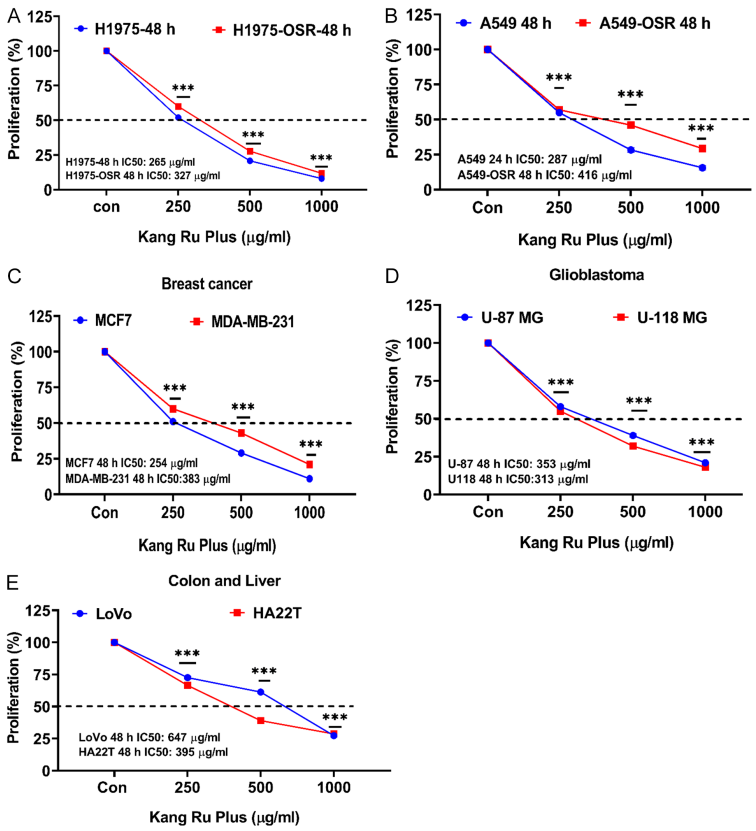

Figure 1. Kang Ru Plus inhibits proliferation across multiple human cancer cell lines. Cancer cells were treated with Kang Ru Plus at concentrations of 250, 500, and 1000 μg/ml for 48 hours, and cell proliferation was assessed via MTT assay. A. H1975 and H1975-OSR; B. A549 and A549-OSR (lung adenocarcinoma); C. MCF7 and MDA-MB-231 (breast cancer); D. U-87 MG and U-118 MG (glioblastoma); E. LoVo (colon cancer) and HA22T (hepatocellular carcinoma). These results are expressed as a percentage of viable cells from treated groups compared with control cells; ***P < 0.001.

Results

Kang Ru Plus inhibits proliferation across multiple human cancer cell lines

To assess the anti-proliferative activity of Kang Ru Plus (KR-Plus), a panel of human cancer cell lines was treated with increasing concentrations of the extract (250, 500, and 1000 μg/mL) for 48 h, and cell viability was measured using the MTT assay. The panel included lung adenocarcinoma cells (H1975, H1975-OSR, A549, A549-OSR), breast cancer cells (MCF7, MDA-MB-231), glioblastoma cells (U-87 MG, U-118 MG), colon cancer cells (LoVo), and hepatocellular carcinoma cells (HA22T).

KR-Plus reduced cell viability in a dose-dependent manner across all cell lines, with significant inhibition observed at 500 and 1000 μg/mL (**Figure 1**). Notably, lung adenocarcinoma cells, including osimertinib-resistant derivatives (H1975-OSR and A549-OSR), remained responsive to KR-Plus. The IC_{50} values for H1975 and H1975-OSR cells were 265.3 μg/mL and 327.0 μg/mL, respectively, while A549 and A549-OSR cells exhibited IC_{50} values of 287.0 μg/mL and 416.3 μg/mL (**Figure 1A**, **1B**; **Table 1**), indicating preserved sensitivity despite acquired resistance to EGFR-targeted therapy.

Among non-lung cancer models, MCF7 breast cancer cells showed the highest sensitivity (IC_{50} = 254.0 μg/mL), followed by glioblastoma cells U-118 MG (312.7 μg/mL) and U-87 MG (353.3 μg/mL). MDA-MB-231 cells exhibited moderate sensitivity (382.7 μg/mL), whereas LoVo colon cancer cells and HA22T hepatocellular carcinoma cells were comparatively less sensitive, with IC_{50} values of 647.0 μg/mL and 395.0 μg/mL, respectively (**Figure 1C-E**; **Table 1**).

Collectively, these findings demonstrate that KR-Plus exerts broad anti-proliferative effects across diverse cancer cell types, with sustained activity in osimertinib-resistant lung adenocarcinoma models.

Kang Ru Plus restores sensitivity to osimertinib in resistant lung adenocarcinoma cells

To validate the resistant phenotype, the sensitivity of parental H1975 and A549 cells and their osimertinib-resistant derivatives (H1975-OSR and A549-OSR) to osimertinib (OS) was assessed using the MTT assay. Resistant cells exhibited markedly reduced responsiveness across a concentration range of 1.5-20 μM (**Figure 2A**, **2B**). The IC_{50} values for H1975-OSR and A549-OSR were 25.0 μM and 28.0 μM, respectively - approximately ten-fold higher than those of parental H1975 (2.27 μM) and

Table 1. KR-Pus IC_{50} values in various cell lines

Cell/Treatment	IC_{50} μg/ml	STDV	95% CI	
	Mean	±	Lower	Upper
H1975-24 h	388	7.506	369	406.3
H1975-48 h	265.3	5.508	251.7	279
H1975-OSR-24 h	906	7.5	898	915.3
H1975-OSR-48 h	327	8.544	305.8	348.2
A549-24 h	922	6.557	905.7	938.3
A549-48 h	287	8.185	266.7	307.3
A549-OSR-24 h	1014	5.568	1000	1028
A549-OSR-48 h	416.3	8.083	396.3	436.4
U-87 48 h	353.3	7.638	334.4	372.3
U-118 48 h	312.7	8.083	292.6	332.7
MCF7 48 h	254	7.55	235.2	272.8
MDA-MB-231 48 h	382.7	11.59	353.9	411.5
LOVO 48 h	647	16.09	607	687
HA22T 48 h	395	6	380.1	409.9

A549 (3.33 μM) cells (**Table 2**) - confirming successful establishment of drug resistance.

KR-Plus treatment significantly reduced cell viability in both H1975-OSR and A549-OSR cells in a dose- and time-dependent manner (**Figure 2C-F**). Notably, IC_{50} values decreased with prolonged exposure, from 906.0 μg/mL to 327.0 μg/mL in H1975-OSR cells and from 1014.0 μg/mL to 416.3 μg/mL in A549-OSR cells at 24 h and 48 h, respectively (**Table 1**), indicating enhanced growth inhibition over time.

Combination treatment further potentiated anti-proliferative effects. Co-treatment with KR-Plus (250 or 500 μg/mL) and osimertinib significantly reduced cell viability compared with either agent alone, with pronounced effects observed even at low osimertinib concentrations (1.5-5 μM) in both resistant cell lines (**Figure 2G**, **2H**). Consistent with these findings, combination index (CI) analysis using the Chou-Talalay method demonstrated synergistic interactions (CI < 1) across multiple dose combinations, particularly with KR-Plus (250-500 μg/mL) in combination with osimertinib (2.5-5 μM) (**Figure 2I**, **2J**; Supplementary Tables 1, 2).

Collectively, these results demonstrate that KR-Plus enhances the responsiveness of osimertinib-resistant lung adenocarcinoma cells and acts synergistically with EGFR-targeted therapy to suppress tumor cell proliferation in vitro.

Kang Ru Plus suppresses EGFR/PI3K/AKT/ERK/mTOR signaling in resistant lung cancer cells

To elucidate the molecular mechanisms underlying the effects of KR-Plus in resistant lung adenocarcinoma cells, we examined its impact on EGFR-associated signaling pathways in H1975-OSR and A549-OSR cells. Western blot analysis revealed that KR-Plus treatment, either alone or in combination with osimertinib, markedly reduced the phosphorylation of EGFR and its downstream effectors, including PI3K, AKT, ERK, and mTOR in H1975-OSR cells (**Figure 3A**).

These findings were further supported by immunofluorescence analysis in A549-OSR cells, which showed a clear reduction in phosphorylated EGFR (p-EGFR) signal intensity following KR-Plus treatment compared with control cells. Notably, the greatest suppression of p-EGFR was observed in the combination treatment groups (**Figure 3B**).

To further assess the effect of KR-Plus on EGFR activation, cells were stimulated with NSC 228155, a known EGFR activator. Despite pharmacological activation of EGFR, KR-Plus maintained its inhibitory effect on EGFR phosphorylation and downstream signaling components, including PI3K, AKT, and ERK (**Figure 3C**).

These findings suggest that KR-Plus inhibits EGFR-driven signaling upstream of, or independently from, receptor activation, thereby overcoming compensatory pathway activation associated with osimertinib resistance.

Kang Ru Plus induces cell-cycle arrest and apoptosis in resistant lung adenocarcinoma cells

To further elucidate the mechanisms underlying KR-Plus-mediated growth inhibition, we examined DNA damage responses, cell-cycle

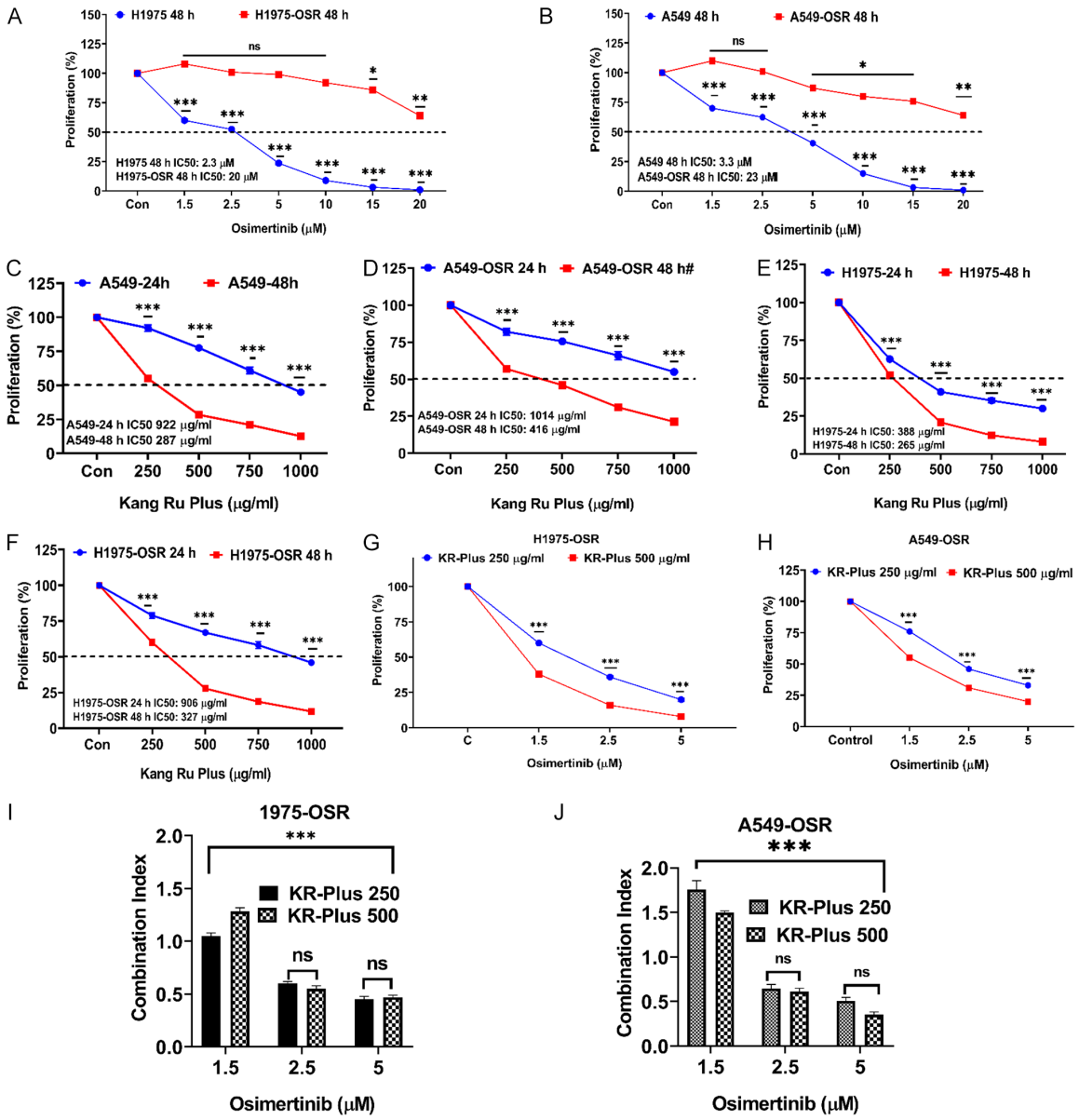

Figure 2. Kang Ru Plus restores sensitivity to osimertinib in resistant lung adenocarcinoma cells. Cell proliferation was evaluated by MTT assay following treatment with osimertinib or Kang Ru Plus (KR-Plus) for 24 or 48 h. A, B. Parental H1975 and A549 cells and their osimertinib-resistant derivatives, H1975-OSR and A549-OSR, were treated with increasing concentrations of osimertinib (1.5-20 μM) for 48 h to confirm the resistant phenotype. C-F. A549, A549-OSR, H1975, and H1975-OSR cells were treated with KR-Plus (250-1000 μg/mL) for 24 or 48 h. G, H. A549-OSR and H1975-OSR cells were treated with osimertinib (1.5-5 μM) in combination with KR-Plus (250 or 500 μg/mL). I, J. Combination index (CI) values were calculated using the Chou-Talalay method to evaluate drug interactions between KR-Plus and osimertinib. CI < 1 indicates synergism, CI = 1 indicates an additive effect, and CI > 1 indicates antagonism. Data are expressed as percentage cell viability relative to untreated control cells. ns, not significant; ***P < 0.001.

regulators, and apoptosis-related proteins in H1975-OSR lung adenocarcinoma cells.

Western blot analysis showed that KR-Plus treatment, either alone or in combination with osimertinib (OS), increased the expression of DNA damage and cell-cycle regulatory markers, including γH2AX, p53, p21, and p16, compared with control cells (**Figure 4A**). These changes were accompanied by modulation of apoptosis-associated proteins, characterized by upregulation of pro-apoptotic markers (BAX, cleaved

Table 2. Osimertinib IC_{50} values in A549, A549-OSR, H1975, H1975-OSR at 48 h treatment

Cell	IC_{50} μM	STDV	95% CI	
	Mean	±	Lower	Upper
A549	3.333	0.4509	2.213	4.453
A549-OSR	28	2	23.03	32.97
H1975	2.267	0.4509	1.147	3.387
H1975-OSR	25	2	20.03	29.97

caspase-3, and cleaved PARP) and downregulation of the anti-apoptotic protein Bcl-2 and the proliferation marker PCNA (**Figure 4B**).

Consistent with these findings, immunofluorescence analysis of PCNA in A549-OSR cells revealed a marked reduction in nuclear PCNA signal intensity following KR-Plus treatment, with the greatest decrease observed in the combination groups (**Figure 4C**).

Flow cytometric analysis using Annexin V/PI staining demonstrated a significant increase in apoptotic cell populations following KR-Plus treatment, particularly under combination conditions (**Figure 4D**). Quantitative analysis confirmed a dose-dependent increase in total apoptosis. In parallel, cell-cycle analysis revealed an accumulation of cells in the sub-G1 phase after KR-Plus exposure, consistent with apoptotic DNA fragmentation (**Figure 4E**).

These findings suggest that KR-Plus-induced apoptosis is mediated, at least in part, through activation of DNA damage-associated checkpoint signaling and mitochondrial apoptotic pathways.

Metabolite profiling and network pharmacology reveal multi-target mechanisms of Kang Ru Plus

To characterize the phytochemical composition of Kang Ru Plus (KR-Plus), untargeted metabolite profiling was performed using ultra-high-performance liquid chromatography coupled with quadrupole time-of-flight mass spectrometry (UHPLC-QTOF-MS). Metabolites were annotated based on accurate mass matching and MS/MS fragmentation patterns using public databases, including HMDB, METLIN, and MassBank.

LC-MS analysis identified more than 20 phytochemicals in the KR-Plus extract, encompassing flavonoids (e.g., quercetin derivatives, apigenin glucuronide, isoorientin), phenolic acids (e.g., syringic acid), lignans (e.g., syringaresinol), and terpenoid-related compounds such as [6]-shogaol and steviol (**Figure 5A**; Supplementary Tables 3, 4). Several prominent metabolites were detected, including quercetin-3,7,3',4'-tetramethyl ether, wogonoside, isoquercetin, apigenin 7-glucuronide, pyridoxal, and n-hexadecanoic acid.

To explore potential molecular targets, predicted interactions between identified metabolites and human proteins were analyzed using SwissTargetPrediction. Network pharmacology analysis highlighted key regulatory proteins implicated in cancer-related pathways, including EGFR, PI3K, AKT1, MAPK1/3, mTOR, TP53, CASP3, and PARP1 (**Figure 5B**). Pathway enrichment analysis based on the KEGG 2021 Human database revealed significant associations with pathways involved in non-small cell lung cancer, apoptosis, and cell-cycle regulation (**Figure 5C-E**).

Molecular docking analysis further demonstrated favorable binding interactions between selected KR-Plus metabolites and the EGFR kinase domain. Compounds such as pyridoxal, n-hexadecanoic acid, and quercetin derivatives were predicted to interact within the ATP-binding pocket through hydrogen bonding and hydrophobic interactions (**Figure 5F-H**).

These multi-level interactions align with the observed suppression of EGFR/PI3K/AKT/ERK signaling and induction of apoptosis, providing mechanistic support for the synergistic effects of KR-Plus in overcoming osimertinib resistance.

Kang Ru Plus enhances osimertinib antitumor efficacy in xenograft models

To evaluate the in vivo antitumor activity of Kang Ru Plus (KR-Plus), H1975-OSR xenograft models were established in BALB/c nude mice. Body weight remained stable across all groups throughout the treatment period, indicating no apparent systemic toxicity (**Figure 6A**).

Combination treatment with KR-Plus (500 mg/kg/day) and osimertinib (25 mg/kg/day) significantly suppressed tumor growth compared with vehicle control and monotherapy groups. Tumor volume measurements revealed pro-

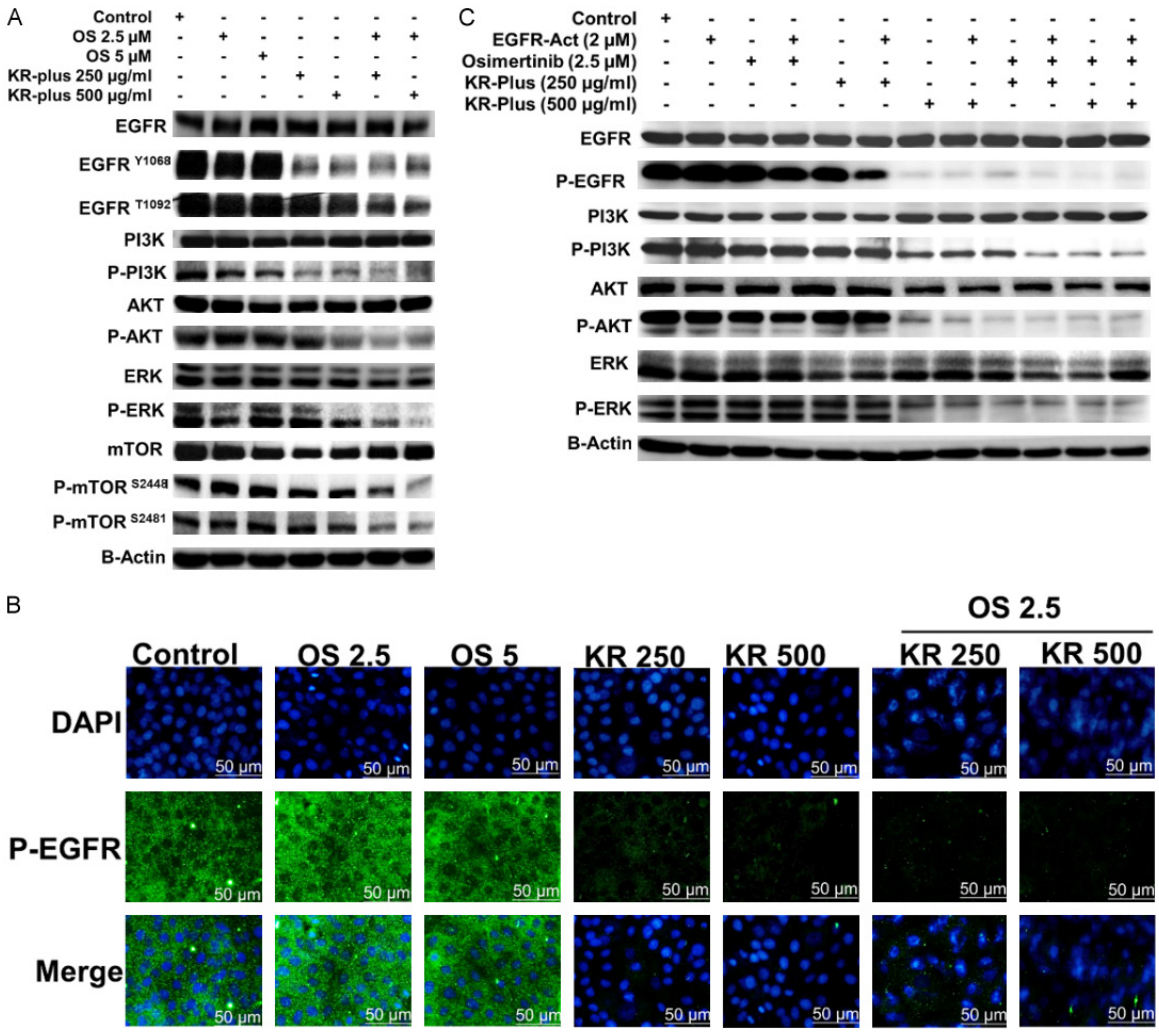

Figure 3. Kang Ru Plus suppresses EGFR/PI3K/AKT/ERK/mTOR signaling in resistant lung cancer cells. (A) H1975-OSR cells were treated with osimertinib (OS, 2.5 and 5 μM), Kang Ru Plus (KR-Plus, 250 and 500 μg/ml), or their combination, followed by western blot analysis of EGFR pathway proteins. (B) Immunofluorescence staining of phosphorylated EGFR (p-EGFR, green) and nuclear counterstaining with DAPI (blue) in A549-OSR cells treated as in (A). (C) Western blot validation of dose-dependent inhibition of EGFR signaling by KR-Plus (250-500 μg/ml), alone or in combination with Osimertinib (2.5 μM), in the presence of the EGFR activator NSC 228155 (2 μM). β-Actin served as the loading control. Representative images are shown; scale bar = 50 nm.

gressive inhibition beginning in the second week of treatment, with the combination group showing the greatest reduction by day 30 (**Figure 6B**).

Kaplan-Meier survival analysis demonstrated a significant survival benefit in the combination group relative to KR-Plus or osimertinib alone (**Figure 6C**). Consistent with the safety profile, serum biochemical markers - including blood urea nitrogen (BUN), glutamate oxaloacetate transaminase (GOT), glutamate pyruvate transaminase (GPT), and total bilirubin (T-Bil) - remained comparable across all groups (**Figure 6D**).

Excised tumors from the combination group were visibly smaller than those from control or monotherapy groups (**Figure 6E**), and tumor weights were significantly reduced (**Figure 6F**). Molecular analysis of tumor lysates showed decreased phosphorylation of EGFR and AKT, reduced expression of the proliferation marker PCNA, and increased levels of cleaved caspase-3 (**Figure 6G**). Immunohistochemical analysis further confirmed reduced p-EGFR and PCNA expression, along with increased cleaved caspase-3 and TUNEL-positive cells in tumor tissues from the combination group (**Figure 6H**).

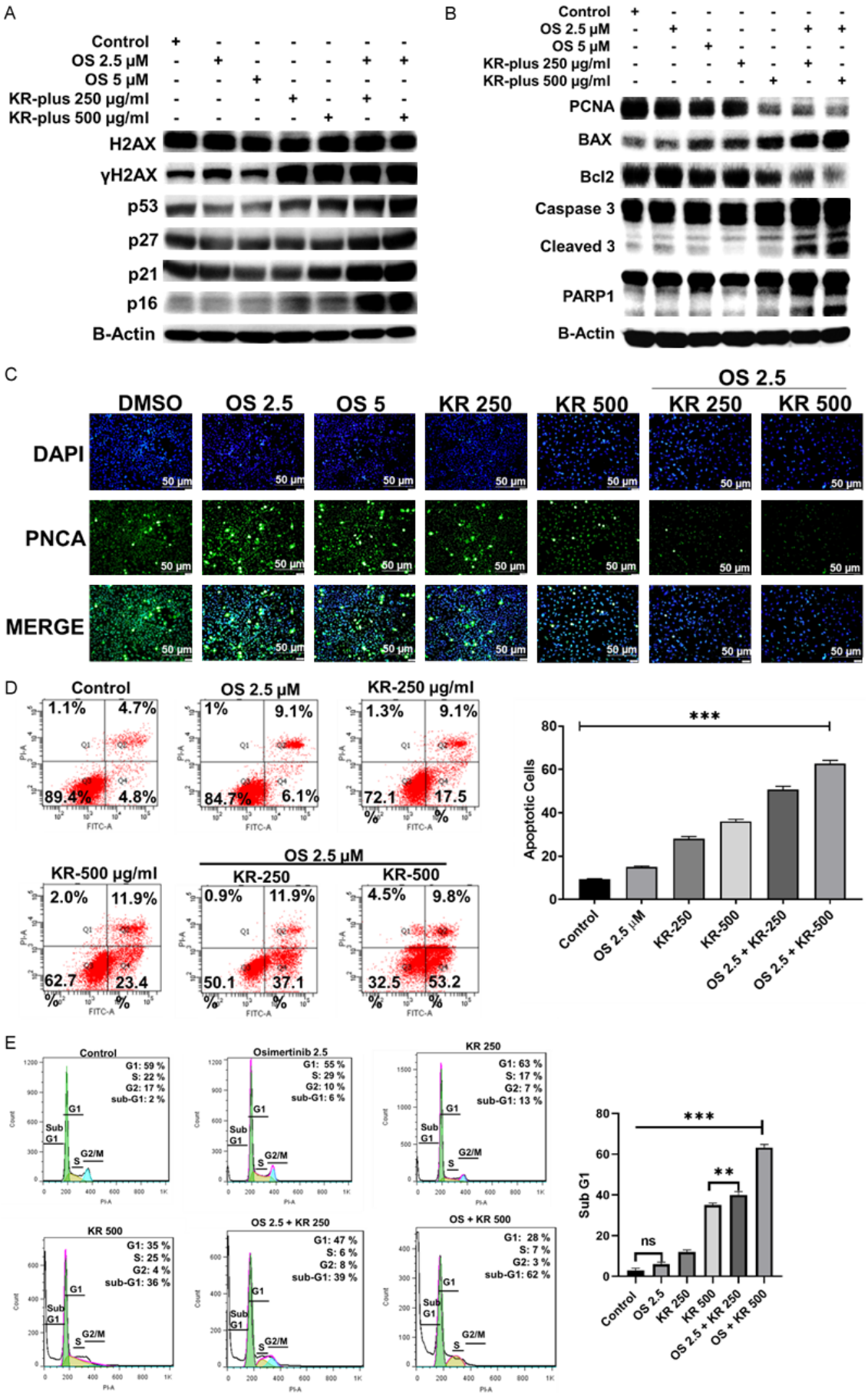
A
Control
OS 2.5 μM
OS 5 μM
KR-plus 250 μg/ml
KR-plus 500 μg/ml
H2AX
γH2AX
p53
p27
p21
p16
B-Actin
B
Control
OS 2.5 μM
OS 5 μM
KR-plus 250 μg/ml
KR-plus 500 μg/ml
PCNA
BAX
Bcl2
Caspase 3
Cleaved 3
PARP1
B-Actin
C
DMSO
OS 2.5
OS 5
KR 250
KR 500
OS 2.5
KR 250
KR 500
DAPI
PNCA
MERGE
50 μm
D
Control
OS 2.5 μM
KR-250 μg/ml
KR-500 μg/ml
OS 2.5 μM
KR-250
KR-500
1.1%
4.7%
89.4%
4.8%
1%
9.1%
84.7%
6.1%
1.3%
9.1%
72.1
17.5
2.0%
11.9%
62.7
23.4
0.9%
11.9%
50.1
37.1
4.5%
9.8%
32.5
53.2
FITC-A
Apoptotic Cells
***
Control
OS 2.5 μM
KR-250
KR-500
OS 2.5 + KR-250
OS 2.5 + KR-500
E
Control
G1: 59 %
S: 22 %
G2: 17 %
sub-G1: 2 %
Osimertinib 2.5
G1: 55 %
S: 29 %
G2: 10 %
sub-G1: 6 %
KR 250
G1: 63 %
S: 17 %
G2: 7 %
sub-G1: 13 %
KR 500
G1: 35 %
S: 25 %
G2: 4 %
sub-G1: 36 %
OS 2.5 + KR 250
G1: 47 %
S: 6 %
G2: 8 %
sub-G1: 39 %
OS + KR 500
G1: 28 %
S: 7 %
G2: 3 %
sub-G1: 62 %
G1
Sub G1
S
G2/M
Count
PI-A
Sub G1
***
**
ns
Control
OS 2.5
KR 250
KR 500
OS 2.5 + KR 250
OS + KR 500

Figure 4. Kang Ru Plus induces cell-cycle arrest and apoptosis in resistant lung adenocarcinoma cells. (A) Western blot analysis of DNA damage and cell cycle regulatory proteins (γH2AX, p53, p21, p16) in H1975-OSR cells treated with Osimertinib (OS, 2.5 and 5 μM), Kang Ru Plus (KR-Plus, 250 and 500 μg/ml), or their combination. (B) Western blot analysis of apoptosis-related proteins (BAX, Bcl-2, Caspase-3, PARP, PCNA) under the same treatment conditions. (C) Immunofluorescence staining of PCNA (green) with nuclear counterstaining by DAPI (blue) in A549-OSR cells treated as in (A). (D) Annexin V/PI staining followed by flow cytometry analysis of apoptosis in H1975-OSR cells, with quantification of apoptotic populations. (E) Cell cycle distribution analysis by flow cytometry in H1975-OSR cells (right panel), with quantification of the sub-G1 population (left panel). β-Actin served as the loading control. Representative images are shown; scale bar = 50 nm. Data are presented as mean ± SD; ns: not significant, **P < 0.01, ***P < 0.001.

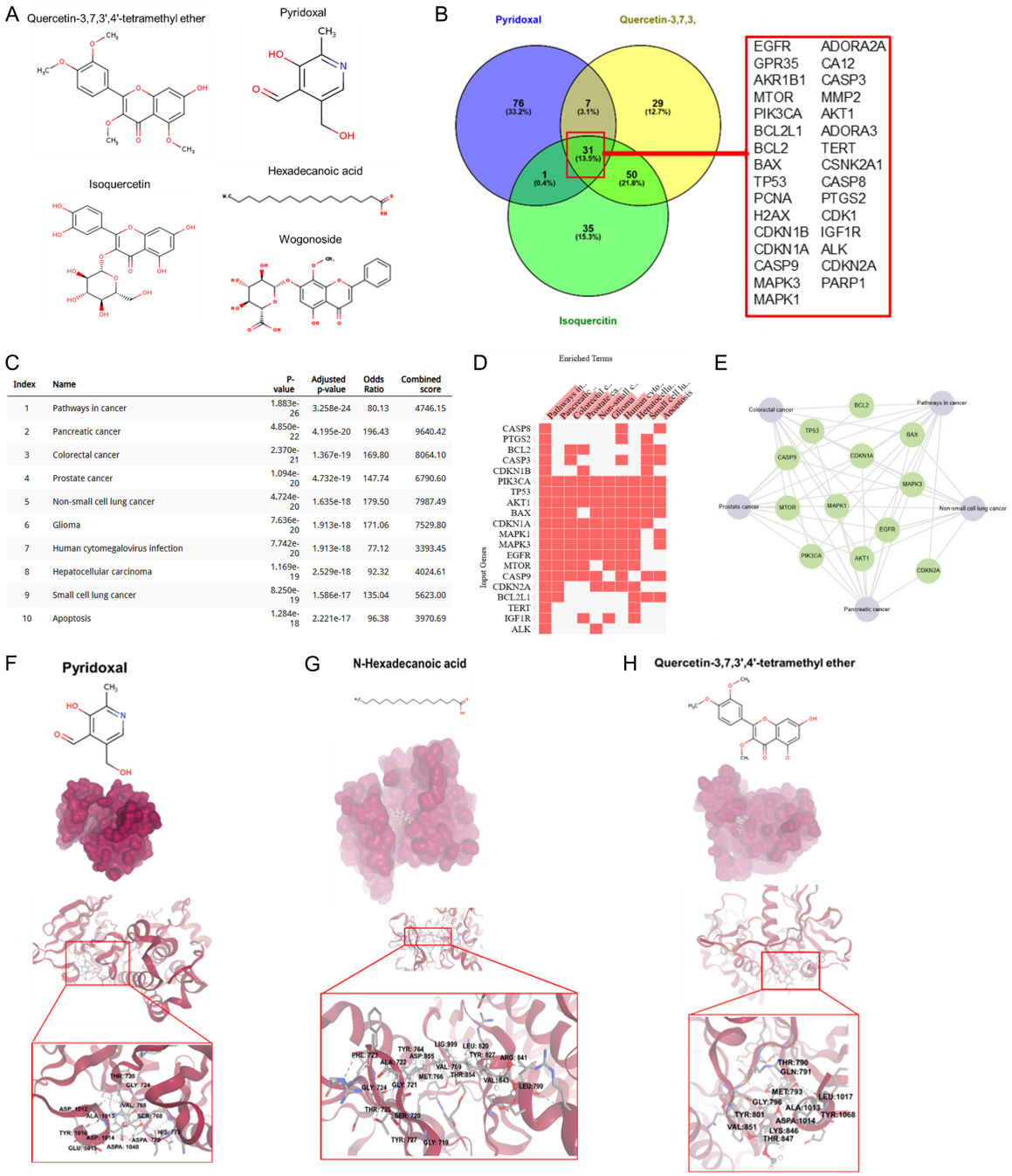

Figure 5. Metabolite profiling and network pharmacology reveal multi-target mechanisms of Kang Ru Plus. A. Representative chemical structures of key KR-Plus metabolites identified by UHPLC-QTOF-MS, including quercetin-3,7,3',4'-tetramethyl ether, pyridoxal, Isoquercetin, n-Hexadecanoic acid, and wogonoside. B. Venn diagram show-

ing predicted target overlap among pyridoxal, quercetin-3,7,3', and Isoquercetin. C. KEGG pathway enrichment analysis of predicted targets, with top-ranked pathways including NSCLC, apoptosis, and multiple solid tumors. D. Heatmap of enriched genes across cancer-related pathways, including CASP8, CDKN1A, MAPK1, and TP53. E. Protein-protein interaction network of KR-Plus targets, showing central nodes such as EGFR, AKT1, MAPK1, TP53, and BAX. F-H. Molecular docking simulations of KR-Plus metabolites with EGFR. Binding site visualizations show hydrogen bonding, hydrophobic interactions, cation-π interactions, and π-π stacking within ATP-binding pockets, supporting direct modulation of survival signaling.

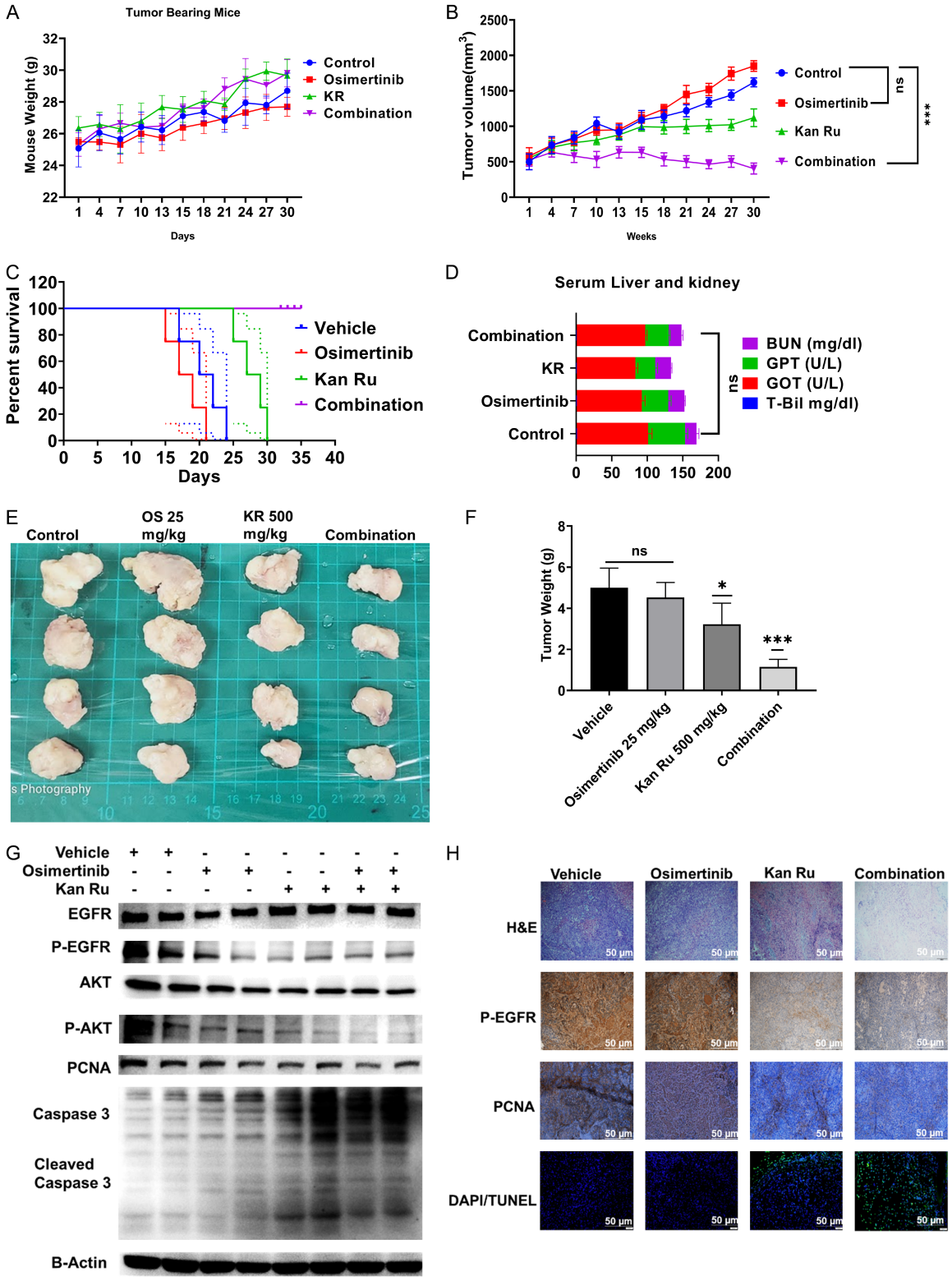

Figure 6. Kang Ru Plus enhances osimertinib antitumor efficacy in xenograft models. A. Monitoring of animal body weight throughout the treatment period. B. Tumor volume measurements during the treatment period. C. Kaplan-Meier survival analysis of tumor-bearing mice across treatment groups. D. Serum biochemical analysis of liver and kidney function markers (BUN, GOT, GPT, T-Bil) at endpoint. E. Gross tumor size from each group at the end of treatment. F. Tumor weight at endpoint. G. Western blot analysis of EGFR pathway proteins, proliferation marker PCNA, and apoptosis marker cleaved Caspase-3. β-actin served as loading control. H. Immunohistochemical staining of tumor tissues for H&E, p-EGFR, PCNA, cleaved Caspase-3 and Tunel assay. Representative images shown; scale bar = 50 μm. Data are expressed as mean ± SD. Statistical significance: ns = not significant, *P < 0.05, ***P < 0.001.

Collectively, these in vivo findings corroborate the in vitro data, supporting a multi-target mechanism by which KR-Plus enhances EGFR inhibition, suppresses tumor proliferation, and promotes apoptosis in resistant tumors.

Discussion

Acquired resistance EGFR tyrosine kinase inhibitors remains a major challenge in the treatment of EGFR-mutant NSCLC. Although third-generation inhibitors such as osimertinib have significantly improved clinical outcomes, tumor cells frequently develop adaptive resistance through activation of compensatory signaling pathways, including PI3K/AKT, MAPK/ERK, and mTOR cascades [4, 5, 29-31]. Sustained activation of these pathways enables cancer cells to maintain proliferative and survival signaling despite EGFR inhibition, thereby facilitating therapeutic escape. Consequently, therapeutic strategies capable of simultaneously targeting multiple oncogenic signaling networks have gained increasing attention as a means to overcome resistance to targeted therapies.

In the present study, we demonstrate that the multi-herb formulation KR-Plus exerts anti-proliferative effects across multiple cancer cell models and significantly enhances the cytotoxic efficacy of osimertinib in drug-resistant lung adenocarcinoma cells. These findings are consistent with previous studies showing that natural products and plant-derived compounds can synergize and sensitize cancer cells to targeted therapies through modulation of key oncogenic signaling pathways [8, 10, 19, 32-35].

Mechanistically, our data show that KR-Plus markedly reduces phosphorylation of EGFR and its downstream effectors, including PI3K, AKT, ERK, and mTOR, in osimertinib-resistant lung adenocarcinoma cells. Importantly, this inhibitory effect was maintained even in the presence of the EGFR activator NSC 228155, indicating that KR-Plus does not act solely at the level of receptor inhibition but may interfere with signaling at multiple nodes within the EGFR pathway. Similar effects have been reported for several medicinal plant-derived compounds. For example, quercetin and related flavonoids have been reported to inhibit EGFR-mediated signaling and promote apoptosis by suppressing the EGFR/ERK axis in various cancer models [8, 9]. Similarly, apigenin has been shown to enhance the antitumor activity of EGFR inhibitors by attenuating downstream EGFR signaling [10]. In addition, extracts of *Houttuynia cordata* have been shown to inhibit the PI3K/AKT/mTOR pathway and suppress cancer cell growth [36], while bioactive constituents of *Lycium barbarum* attenuate ERK and AKT signaling associated with tumor progression [35]. Together, these observations support the concept that phytochemical modulation of EGFR signaling networks can improve the efficacy of targeted anticancer therapies. The signaling suppression observed in this study is therefore consistent with the known pharmacological properties of bioactive constituents present in the KR-Plus formulation. This multi-level interference may be particularly important in overcoming compensatory signaling reactivation associated with acquired resistance to EGFR-targeted therapies.

From a clinical and biological perspective, lung adenocarcinoma cells harboring wild-type EGFR, such as A549, are generally less responsive to osimertinib compared with EGFR-mutant models. The modest inhibition of downstream signaling observed in A549 and A549-OSR cells likely reflects partial suppression of basal EGFR activity or broader network-level effects rather than mutation-dependent sensitivity. Previous studies suggest that EGFR-targeted agents may exert limited effects in EGFR wild-type cells through off-target kinase interactions or modulation of interconnected signaling pathways [37, 38]. In this study, mechanistic conclusions regarding resistance are primarily supported by the EGFR-mutant H1975/H1975-OSR model, which more closely reflects the clinical

context of osimertinib sensitivity and acquired resistance. The A549/A549-OSR system was included to assess whether KR-Plus exerts broader, mutation-independent effects on oncogenic signaling networks. Such network-level modulation may be particularly advantageous in overcoming heterogeneous resistance mechanisms that extend beyond EGFR mutation status [3].

In addition to inhibiting survival signaling, KR-Plus induced cell-cycle arrest and apoptosis in resistant lung adenocarcinoma cells. Increased expression of γH2AX, p53, p21, and p16 indicates activation of DNA damage-associated checkpoint pathways that restrict cell proliferation. Concurrently, upregulation of BAX, cleaved caspase-3, and cleaved PARP, together with downregulation of Bcl-2 and PCNA, supports activation of intrinsic apoptotic pathways. Similar effects have been reported for flavonoids such as quercetin derivatives, which promote mitochondrial apoptosis through modulation of the BAX/Bcl-2 balance and activation of caspase cascades [8, 34]. These findings suggest that the enhanced cytotoxicity observed with KR-Plus and osimertinib results from coordinated inhibition of survival signaling and induction of apoptosis.

Phytochemical profiling revealed that KR-Plus contains a diverse array of bioactive metabolites, including flavonoids, phenolic acids, and terpenoid derivatives. Compounds such as isoquercetin, apigenin derivatives, and wogonoside have been reported to regulate oncogenic signaling pathways involved in tumor progression and drug resistance [10, 32, 33, 39-42]. The presence of multiple bioactive constituents suggests that the pharmacological effects of KR-Plus may arise from synergistic or complementary interactions among these metabolites. Consistent with this, polyherbal formulations have been shown to modulate multiple oncogenic pathways simultaneously, including STAT3, PI3K/AKT, and MAPK cascades, thereby enhancing the efficacy of conventional anticancer therapies [18, 20-22].

Network pharmacology and molecular docking analyses further supported a multi-target mechanism. Predicted interactions between KR-Plus metabolites and key oncogenic regulators - including EGFR, AKT1, MAPK1/3, mTOR, TP53, and CASP3 - highlight the breadth of potential targets. Pathway enrichment analysis identified significant associations with NSCLC progression, apoptosis, and cell-cycle regulation. Docking simulations suggested favorable interactions between selected metabolites and the EGFR kinase domain, indicating possible direct modulation of receptor activity. These findings are consistent with growing evidence that multi-component natural product formulations act through coordinated regulation of interconnected signaling networks rather than a single molecular target [20, 43, 44].

The in vivo xenograft data further support the therapeutic potential of KR-Plus. Combination treatment with KR-Plus and osimertinib significantly suppressed tumor growth and improved survival compared with monotherapy, without detectable systemic toxicity. Body weight remained stable and serum biochemical markers were unchanged, indicating an acceptable safety profile. These findings align with previous reports showing that herbal formulations can enhance the efficacy of targeted therapies while maintaining low toxicity [20, 22, 45], and highlight the potential of KR-Plus as a complementary strategy in resistant NSCLC.

Despite these promising findings, several limitations should be considered. Although the experimental models provide valuable mechanistic insights, they do not fully capture the complexity of human tumors and the tumor microenvironment. In addition, the relative contributions and interactions of individual phytochemicals within KR-Plus remain to be defined. In the in vivo studies, although humane monitoring criteria were applied and no overt toxicity was observed, tumor burden reached levels that may exceed current best-practice thresholds in some settings. Future studies will incorporate earlier intervention time points and stricter tumor size limits (e.g., ≤150-200 mm^3) to further refine experimental design and enhance animal welfare. Additional studies integrating metabolomics-guided fractionation, pharmacokinetic analysis, and clinical investigation will be essential to clarify the translational potential of this formulation. Establishing bioactive markers and standardized quality control measures will also be critical for clinical development.

In conclusion, KR-Plus exerts multi-target pharmacological effects by suppressing EGFR-

associated survival signaling, inducing apoptosis, and enhancing sensitivity to osimertinib in resistant lung adenocarcinoma models. By integrating phytochemical profiling, network pharmacology, and in vivo validation, this study provides mechanistic insight into how multi-component herbal formulations may serve as complementary strategies to overcome resistance to EGFR-targeted therapies. These findings support further translational and clinical evaluation of KR-Plus in the management of osimertinib-resistant NSCLC.

Acknowledgements

This study project was supported by China medical University, Taichung Taiwan and Hualien Tzu Chi Hospital, Buddhist Tzu Chi Medical Foundation. All the experiments were done at China Medical University in Dr. Chih-Yang Huang's laboratory.

Disclosure of conflict of interest

None.

Abbreviations

AKT, protein kinase B; ANOVA, analysis of variance; BAX, Bcl-2-associated X protein; Bcl-2, B-cell lymphoma 2; EGFR, epidermal growth factor receptor; ERK, extracellular signal-regulated kinase; KR-Plus, Kang Ru Plus; LC-MS, liquid chromatography-mass spectrometry; MAPK, mitogen-activated protein kinase; mTOR, mechanistic target of rapamycin; MTT, 3-(4,5-dimethylthiazol-2-yl)-2,5-diphenyltetrazolium bromide; NSCLC, non-small cell lung cancer; OS, osimertinib; PARP, poly (ADP-ribose) polymerase; PCNA, proliferating cell nuclear antigen; PI3K, phosphoinositide 3-kinase; TCM, Traditional Chinese Medicine; UHPLC-QTOF-MS, ultra-high-performance liquid chromatography-quadrupole time-of-flight mass spectrometry.

Address correspondence to: Shinn-Zong Lin, Department of Neurosurgery, Hualien Tzu Chi Hospital, Hualien, Taiwan. Tel: +886-3-8561825 Ext. 15930; Fax: +886-4-22032295; E-mail: shinnzong@yahoo.com.tw; Dr. Chih-Yang Huang, Cardiovascular and Mitochondrial Related Disease Research Center, Hualien Tzu Chi Hospital, Buddhist Tzu Chi Medical Foundation, Hualien, Taiwan. Tel: +886-3-8561825 Ext. 15930; Fax: +886-4-22032295; E-mail: cyhuang@mail.cmu.edu.tw

References

[1] Siegel RL, Kratzer TB, Wagle NS, Sung H and Jemal A. Cancer statistics, 2026. CA Cancer J Clin 2026; 76: e70043.

[2] Tang ZH, Cao WX, Su MX, Chen X and Lu JJ. Osimertinib induces autophagy and apoptosis via reactive oxygen species generation in non-small cell lung cancer cells. Toxicol Appl Pharmacol 2017; 321: 18-26.

[3] Liao YY, Tsai CL and Huang HP. Optimizing osimertinib for NSCLC: targeting resistance and exploring combination therapeutics. Cancers 2025; 17: 459.

[4] Leonetti A, Sharma S, Minari R, Perego P, Giovannetti E and Tiseo M. Resistance mechanisms to osimertinib in EGFR-mutated non-small cell lung cancer. Br J Cancer 2019; 121: 725.

[5] Wang R, Chen Y, Li L, Zhang L and Zhang S. Osimertinib acquired resistance among patients with EGFR-mutated NSCLC: from molecular mechanisms to clinical therapeutic strategies. Cancer Drug Resistance 2025; 8: 61.

[6] Wu L, Ke L, Zhang Z, Yu J and Meng X. Development of EGFR TKIs and options to manage resistance of third-generation EGFR TKI osimertinib: conventional ways and immune checkpoint inhibitors. Front Oncol 2020; 10: 602762.

[7] Chhouri H, Alexandre D and Grumolato L. Mechanisms of acquired resistance and tolerance to EGFR targeted therapy in non-small cell lung cancer. Cancers 2023; 15: 504.

[8] Liu Y, Li Y, Jiang Y, Zheng X, Wang T, Li J, Zhang B, Zhu J, Wei X, Huang R, Zhang Y and Jin Q. Quercetin promotes apoptosis of gastric cancer cells through the EGFR-ERK signaling pathway. J Food Biochem 2024; 2024: 9945178.

[9] Lee J, Han SI, Yun JH and Kim JH. Quercetin 3-O-glucoside suppresses epidermal growth factor-induced migration by inhibiting EGFR signaling in pancreatic cancer cells. Tumour Biol 2015; 36: 9385-9393.

[10] Hu WJ, Liu J, Zhong LK and Wang J. Apigenin enhances the antitumor effects of cetuximab in nasopharyngeal carcinoma by inhibiting EGFR signaling. Biomed Pharmacother 2018; 102: 681-688.

[11] Gao Q and Lu Y. Pharmacological and bioactive properties of Artemisia argyi H. Lév. & Vaniot essential oil: a review. Front Pharmacol 2026; 16: 1664658.

[12] Lu Y, Jiang Y, Ling L, Zhang Y, Li H and Chen D. Beneficial effects of Houttuynia cordata polysaccharides on "two-hit" acute lung injury and endotoxic fever in rats associated with anti-complementary activities. Acta Pharm Sin B 2017; 8: 218.

[13] Mao X, Wu LF, Guo HL, Chen WJ, Cui YP, Qi Q, Li S, Liang WY, Yang GH, Shao YY, Zhu D, She GM, You Y and Zhang LZ. The genus phyllanthus: an ethnopharmacological, phytochemical, and pharmacological review. Evid Based Complement Alternat Med 2016; 2016: 7584952.
[14] Rafiq S, Hao H, Ijaz M and Raza A. Pharmacological effects of houttuynia cordata thunb (H. cordata): a comprehensive review. Pharmaceuticals 2022; 15: 1079.
[15] Rao YK, Fang SH, Hsieh SC, Yeh TH and Tzeng YM. The constituents of Anisomeles indica and their anti-inflammatory activities. J Ethnopharmacol 2009; 121: 292-296.
[16] Zhang T, Alexa EA, Liu G, Berisha A, Walsh R and Kelleher R. Lycium barbarum for health and longevity: a review of its biological significance. Obesities 2025; 5: 35.
[17] Han S, Kim H, Lee MY, Lee J, Ahn KS, Ha IJ and Lee SG. Anti-cancer effects of a new herbal medicine psy by inhibiting the STAT3 signaling pathway in colorectal cancer cells and its phytochemical analysis. Int J Mol Sci 2022; 23: 14826.
[18] Kim J, Kim HY, Hong S, Shin S, Kim YA, Kim NS and Bang OS. A new herbal formula BP10A exerted an antitumor effect and enhanced anticancer effect of irinotecan and oxaliplatin in the colon cancer PDTX model. Biomed Pharmacother 2019; 116: 108987.
[19] Zhang L, Gong Y, Zhang L, Liang B, Xu H, Hu W, Jin Z, Wu X, Chen X, Li M, Shi L, Shi Y, Li M, Huang Y, Wang Y and Yang L. Gou Qi Zi inhibits proliferation and induces apoptosis through the PI3K/AKT1 signaling pathway in non-small cell lung cancer. Front Oncol 2022; 12: 1034750.
[20] Zhang YN, Wu ZC, Yu HY, Wang HX, Liu G, Wang SJ and Ji XM. Chinese herbal medicine Wenxia Changfu formula reverses cell adhesion-mediated drug resistance via the integrin β1-PI3K-AKT pathway in lung cancer. J Cancer 2019; 10: 293.
[21] Zheng T, Que Z, Jiao L, Kang Y, Gong Y, Yao J, Ma C, Bi L, Dong Q, Zhao X and Xu L. Herbal formula YYJD inhibits tumor growth by inducing cell cycle arrest and senescence in lung cancer. Sci Rep 2017; 7: 4984.
[22] Yang W, Kang Y, Zhao Q, Bi L, Jiao L, Gu Y, Lu J, Yao J, Zhou D, Sun J, Zhao X and Xu L. Herbal formula Yangyinjiedu induces lung cancer cell apoptosis via activation of early growth response 1. J Cell Mol Med 2019; 23: 6193.
[23] Munyembaraga V, Mhone TG, Yu YL, Chen MC, Kuo CH, Hsieh DJY, Lin KH, Ho TJ, Kuo WW and Huang CY. MiR-493-3p suppresses the DPY-30 histone methyltransferase complex regulatory subunit to attenuate gefitinib resistance in lung cancer. Transl Oncol 2025; 63: 102570.
[24] Mhone TG, Chen MC, Kuo CH, Shih TC, Yeh CM, Wang TF, Chen RJ, Chang YC, Kuo WW and Huang CY. Daidzein synergizes with gefitinib to induce ROS/JNK/c-Jun activation and inhibit EGFR-STAT/AKT/ERK pathways to enhance lung adenocarcinoma cells chemosensitivity. Int J Biol Sci 2022; 18: 3636-3652.
[25] Chang CM, Wang WJ, Mhone TG, Ho WK, Chen CJ, Ng SSC, Li CC, Kuo CH, Huang CY and Kuo WW. Diallyl trisulfide enhances doxorubicin chemosensitivity by inhibiting the warburg effect and inducing apoptosis in breast cancer cells. J Cancer 2025; 16: 3283.
[26] Azizah M, Pripdeevech P, Thongkongkaew T, Mahidol C, Ruchirawat S and Kittakoop P. UHPLC-ESI-QTOF-MS/MS-based molecular networking guided isolation and dereplication of antibacterial and antifungal constituents of ventilago denticulata. Antibiotics 2020; 9: 606.
[27] Bugnon M, Röhrig UF, Goullieux M, Perez MAS, Daina A, Michielin O and Zoete V. SwissDock 2024: major enhancements for small-molecule docking with attracting cavities and autodock vina. Nucleic Acids Res 2024; 52: W324-W332.
[28] Chen EY, Tan CM, Kou Y, Duan Q, Wang Z, Meirelles GV, Clark NR and Ma'ayan A. Enrichr: interactive and collaborative HTML5 gene list enrichment analysis tool. BMC Bioinformatics 2013; 14: 128.
[29] Yu L, Bazhenova L, Gold K, Tran L, Hilburn V, Vu P and Patel SP. Clinicopathologic and molecular characteristics of EGFR-mutant lung adenocarcinomas that transform to small cell lung cancer after TKI therapy. Transl Lung Cancer Res 2022; 11: 452-461.
[30] Mancini M, Thomas QD, Bourdel S, Papon L, Bousquet E, Jalta P, La Monica S, Travert C, Alfieri R, Quantin X, Cañamero M and Maraver A. Generation and characterization of a new preclinical mouse model of egfr-driven lung cancer with met-induced osimertinib resistance. Cancers (Basel) 2021; 13: 3441.
[31] Fu K, Xie F, Wang F and Fu L. Therapeutic strategies for EGFR-mutated non-small cell lung cancer patients with osimertinib resistance. J Hematol Oncol 2022; 15: 1-32.
[32] Wei Z, Zheng D, Pi W, Qiu Y, Xia K and Guo W. Isoquercitrin restrains the proliferation and promotes apoptosis of human osteosarcoma cells by inhibiting the Wnt/β-catenin pathway. J Bone Oncol 2023; 38: 100468.
[33] Shui L, Wang W, Xie M, Ye B, Li X, Liu Y and Zheng M. Isoquercitrin induces apoptosis and autophagy in hepatocellular carcinoma cells via AMPK/mTOR/p70S6K signaling pathway. Aging (Albany NY) 2020; 12: 24318.
[34] Jin H, Qiao F, Wang Y, Xu Y and Shang Y. Curcumin inhibits cell proliferation and induces

apoptosis of human non-small cell lung cancer cells through the upregulation of miR-192-5p and suppression of PI3K/Akt signaling pathway. Oncol Rep 2015; 34: 2782-2789.

[35] Sanghavi A, Srivatsa A, Adiga D, Chopra A, Lobo R, Kabekkodu SP, Gadag S, Nayak U, Sivaraman K and Shah A. Goji berry (Lycium barbarum) inhibits the proliferation, adhesion, and migration of oral cancer cells by inhibiting the ERK, AKT, and CyclinD cell signaling pathways: an in-vitro study. F1000Res 2023; 11: 1563.

[36] Chen H, Feng X, Gao L, Mickymaray S, Paramasivam A, Abdulaziz Alfaiz F, Almasmoum HA, Ghaith MM, Almaimani RA and Aziz Ibrahim IA. Inhibiting the PI3K/AKT/mTOR signalling pathway with copper oxide nanoparticles from Houttuynia cordata plant: attenuating the proliferation of cervical cancer cells. Artif Cells Nanomed Biotechnol 2021; 49: 240-249.

[37] Nanamiya R, Saito-Koyama R, Miki Y, Inoue C, Asavasupreechar T, Abe J, Sato I and Sasano H. EphB4 as a novel target for the EGFR-independent suppressive effects of osimertinib on cell cycle progression in non-small cell lung cancer. Int J Mol Sci 2021; 22: 8522.

[38] Lin S, Ruan H, Qin L, Zhao C, Gu M, Wang Z, Liu B, Wang H and Wang J. Acquired resistance to EGFR-TKIs in NSCLC mediates epigenetic downregulation of MUC17 by facilitating NF-κB activity via UHRF1/DNMT1 complex. Int J Biol Sci 2023; 19: 832.

[39] Ujiki MB, Ding X-Z, Salabat MR, Bentrem DJ, Golkar L, Milam B, Talamonti MS, Bell RH, Iwamura T and Adrian TE. Apigenin inhibits pancreatic cancer cell proliferation through G2/M cell cycle arrest. Mol Cancer 2006; 5: 76.

[40] Gonzalez-Mejia ME, Voss OH, Murnan EJ and Doseff AI. Apigenin-induced apoptosis of leukemia cells is mediated by a bimodal and differentially regulated residue-specific phosphorylation of heat-shock protein-27. Cell Death Dis 2010; 1: e64.

[41] Kaewmanee M, Limpaiboon T and Ngernyuang N. Apigenin induces apoptosis and inhibits migration in human cholangiocarcinoma cells. Toxics 2025; 13: 112.

[42] Yang J, Pi C and Wang G. Inhibition of PI3K/Akt/mTOR pathway by apigenin induces apoptosis and autophagy in hepatocellular carcinoma cells. Biomed Pharmacother 2018; 103: 699-707.

[43] Zou JY, Chen QL, Luo XC, Damdinjav D, Abdelmohsen UR, Li HY, Battulga T, Chen HB, Wang YQ and Zhang JY. Natural products reverse cancer multidrug resistance. Front Pharmacol 2024; 15: 1348076.

[44] Jenča A, Mills DK, Ghasemi H, Saberian E, Forood AMK, Petrášová A, Jenčová J, Velisdeh ZJ, Zare-Zardini H and Ebrahimifar M. Herbal therapies for cancer treatment: a review of phytotherapeutic efficacy. Biologics 2024; 18: 229.

[45] Shibu MA, Lin YJ, Chiang CY, Lu CY, Goswami D, Sundhar N, Agarwal S, Islam MN, Lin PY, Lin SZ, Ho TJ, Tsai WT, Kuo WW and Huang CY. Novel anti-aging herbal formulation Jing Si displays pleiotropic effects against aging associated disorders. Biomed Pharmacother 2022; 146: 112427.

Supplementary Table 1. Combination index (CI) analysis using the Chou-Talalay method in A549-OSR cells

KR-Plus	OS (μM)	Viability (%)	Fa	CI	Interpretation
250	1.5	76	0.24	1.87	Antagonism
250	2.5	46	0.54	0.69	Synergy
250	5	33	0.67	0.47	Strong synergy
500	1.5	55	0.45	1.49	Antagonism
500	2.5	31	0.69	0.61	Synergy
500	5	20	0.80	0.38	Strong synergy

Supplementary Table 2. Combination index (CI) analysis using the Chou-Talalay method in H1975-OSR cells

KR-Plus	OS (μM)	Viability (%)	Fa	CI	Interpretation
250	1.5	60	0.40	1.02	Additive
250	2.5	36	0.64	0.62	Synergy
250	5	20	0.80	0.45	Strong synergy
500	1.5	38	0.62	1.28	Antagonism
500	2.5	16	0.84	0.55	Strong synergy
500	5	8	0.92	0.49	Strong synergy

Supplementary Table 3. Annotated metabolites identified by LC-MS/MS

Alignment ID	Rt (min)	m/z (Observed)	Metabolite Name	Adduct Type	Reference m/z	Molecular Formula
127	5.058	177.05472	7-Methoxycoumarin	[M+H]+	177.0546	$C_{10}H_8O_3$
143	1.226	184.06030	4-Pyridoxic acid (w/o MS2)	[M+H]+	184.06039	$C_8H_9NO_4$
177	3.021	199.06020	Syringic acid	[M+H]+	199.0601	$C_9H_{10}O_5$
330	2.692	242.11349	Ritalinic acid (w/o MS2)	[M+H]+	242.1152	$C_{13}H_{17}NO_2$
477	5.435	274.27399	Isopalmitic acid (w/o MS2)	[M+H]+	274.27405	$C_{16}H_{32}O_2$
489	5.790	277.18005	[6]-Shogaol	[M+H]+	277.17981	$C_{17}H_{24}O_3$
595	4.621	301.21552	Steviol	[M+H-H_2O]+	301.21619	$C_{20}H_{30}O_3$
788	6.855	353.10172	Parvisoflavone B	[M+H]+	353.10199	$C_{20}H_{16}O_6$
821	6.777	359.11279	Quercetin-3,7,3',4'-tetramethyl ether	[M+H]+	359.11249	$C_{19}H_{18}O_7$
883	3.504	377.14551	(-)-Riboflavin	[M+H]+	377.1456	$C_{17}H_{20}N_4O_6$
964	4.764	401.15897	Syringaresinol	[M+H-H_2O]+	401.15948	$C_{22}H_{26}O_8$
999	3.886	411.10703	Swertisin	[M+H-H_2O]+	411.10739	$C_{22}H_{22}O_{10}$
1124	1.085	446.15286	Rosuvastatin (w/o MS2)	[M+H]+	446.15439	$C_{22}H_{28}FN_3O_6S$
1126	4.135	447.09259	Apigenin 7-glucuronide	[M+H]+	447.09219	$C_{21}H_{18}O_{11}$
1137	3.590	449.10895	Isoorientin	[M+H]+	449.10779	$C_{21}H_{20}O_{11}$
1179	4.249	461.10699	Wogonoside (w/o MS2)	[M+H]+	461.10779	$C_{22}H_{20}O_{11}$
1191	3.664	463.12286	Swertiajaponin	[M+H]+	463.12	$C_{22}H_{22}O_{11}$
1196	3.208	465.10321	Isoquercitin	[M+H]+	465.10281	$C_{21}H_{20}O_{12}$
1204	6.252	467.19394	Asperglaucide	[M+Na]+	467.19409	$C_{27}H_{28}N_2O_4$
1208	3.912	469.11050	Swertisin (w/o MS2)	[M+H]+	469.10999	$C_{22}H_{22}O_{10}$
1594	3.215	627.15625	Quercetin 3,4'-diglucoside	[M+H]+	627.15558	$C_{27}H_{30}O_{17}$
1710	6.293	699.35553	Gingerglycolipid A (w/o MS2)	[M+H]+	699.3562	$C_{33}H_{56}O_{14}$

Supplementary Table 4. Annotated metabolites with reported anticancer and EGFR-modulating activities

Metabolite Name	Molecular Formula	Reported Anticancer Activity	EGFR/Pathway Modulation	Reference
Quercetin-3,7,3',4'-tetramethyl ether	$C_{19}H_{18}O_7$	Inhibits proliferation, induces apoptosis in NSCLC and breast cancer	Suppresses EGFR phosphorylation and PI3K/AKT	PMID: 29956731
Isoquercitin	$C_{21}H_{20}O_{12}$	Induces apoptosis and cell cycle arrest in lung and colon cancer	Downregulates EGFR and ERK	PMID: 26351552
Apigenin 7-glucuronide	$C_{21}H_{18}O_{11}$	Suppresses tumor growth, enhances chemosensitivity	Inhibits EGFR and MAPK signaling	PMID: 33152472
Isoorientin	$C_{21}H_{20}O_{11}$	Promotes apoptosis and ROS generation in cancer cells	Modulates MAPK/ERK signaling	PMID: 36558992
Wogonoside	$C_{22}H_{20}O_{11}$	Alleviates the proliferation and promotes the apoptosis	Blocks PI3K/Akt signaling pathway	PMID: 40011302
Swertisin	$C_{22}H_{22}O_{10}$	Induction of apoptosis in human pancreatic cancer	Mitochondrial membrane potential	PMID: 23453831
Swertiajaponin	$C_{22}H_{22}O_{11}$	Inhibits skin pigmentation	Inhibited MAPK/MITF signaling	PMID: 29221146
Syringic acid	$C_9H_{10}O_5$	Antioxidant and anti-proliferative effects	Apoptosis and ROS and DNA damage levels	PMID: 33548266
[6]-Shogaol	$C_{17}H_{24}O_3$	Induces apoptosis, inhibits migration in lung and Oral cancer	Downregulates EGFR and PI3K/AKT	PMID: 24282290 PMID: 34644781
Rosuvastatin	$C_{22}H_{28}FN_3O_6S$	Inhibits proliferation and migration in NSCLC	Suppresses RAS MMP and NF-κB	PMID: 23510472
Steviol	$C_{20}H_{30}O_3$	Induces apoptosis and inhibits proliferation osteosarcoma	Induces cell cycle arrest, and apoptotic pathway,	PMID: 29552164